

LINC00167 Regulates RPE Differentiation by Targeting the miR-203a-3p/SOCS3 Axis

Xue Chen,^{1,2} Ruxu Sun,^{1,2} Daidi Yang,¹ Chao Jiang,¹ and Qinghuai Liu¹

¹Department of Ophthalmology, The First Affiliated Hospital of Nanjing Medical University, Nanjing Medical University, Nanjing 210029, China

Increasing evidence has indicated that long non-coding RNAs (lncRNAs) play significant roles in various diseases; however, their roles in age-related macular degeneration (AMD) remain unclear. Dedifferentiation and dysfunction of retinal pigment epithelium (RPE) cells have been shown to contribute to AMD etiology in several studies. Herein, we found that lncRNA LINC00167 was downregulated in RPE-choroid samples of AMD patients and dysfunctional RPE cells, and it was consistently upregulated along with RPE differentiation. *In vitro* study indicated that reduced endogenous LINC00167 expression resulted in RPE dedifferentiation, which was typified by attenuated expression of RPE markers, reduced vascular endothelial growth factor A secretion, accumulation of mitochondrial reactive oxygen species, and interrupted phagocytic ability. Mechanistically, LINC00167 functioned as a sponge for microRNA miR-203a-3p to restore the expression of the suppressor of cytokine signaling 3 (SOCS3), which further inhibited the Janus kinase (JAK)/signal transducer and activator of transcription (STAT) signaling pathway. Taken together, our study demonstrated that LINC00167 showed a protective role in AMD by maintaining RPE differentiation through the LINC00167/miR-203a-3p/SOCS3 axis and might be a potential therapeutic target for AMD.

INTRODUCTION

Retinal pigment epithelium (RPE) is composed of cuboidal, postmitotic, and polarized cells located in the outer retina between photoreceptor outer segments and Bruch's membrane.^{1–3} RPE plays vital roles in maintaining balance of the retinal microenvironment through phagocytosis and digestion of photoreceptor outer segments, participating in the visual cycle, composing the blood-retina barrier with tight junctions, and secreting multiple growth factors essential for endothelial cells.^{1,4} Depletion of RPE function is involved in multiple retinal degenerative diseases, including age-related macular degeneration (AMD).^{1,5–7} AMD is one of the leading causes for vision loss in aged people.⁸ Due to its irreversible progression and unsatisfied treatment effect, AMD severely lowered patients' life quality.^{9,10} According to histopathologic changes in the retina, AMD can be classified in to two categories: nonexudative AMD and neovascular AMD.¹¹ Nonexudative AMD, also known as dry AMD, is characterized by drusen or debris within Bruch's membrane, subretinal deposits, RPE abnormalities, and RPE cell loss.^{12–14} By far, no efficient treatment has been raised for dry AMD. Previous study has

illuminated that RPE dedifferentiation marked by attenuated RPE-characteristic protein is associated with RPE dysfunction in the early stage of AMD.^{1,15} Therefore, investigations into RPE dedifferentiation may help to learn more about AMD pathogenesis and to come up with effective therapy for AMD.

Long non-coding RNAs (lncRNAs) are a class of non-protein-coding transcripts longer than 200 nt.¹⁶ Functions of lncRNAs include co-transcriptional regulation, molecular recruitment to specific loci, RNA-binding titration, and microRNA (miRNA) sponge.^{16,17} lncRNAs could regulate messenger RNA (mRNA) expressions by functioning as a miRNA sponge,^{18,19} and they play regulatory roles in various biological processes, such as tumor genesis, cell differentiation, and epithelial-mesenchymal transition.^{20–22} However, roles of lncRNAs in RPE dedifferentiation remain unclear. In this study, we sought to investigate the function of lncRNA LINC00167 in RPE dedifferentiation.

RESULTS

LINC00167 Is Decreased in AMD

RPE dedifferentiation is an initial pathological event in AMD.^{1,3} We have previously identified the crucial roles of lncRNAs in AMD etiology.¹⁴ Herein, we analyzed the expression of lncRNA LINC00167 (ENST00000530583) in human-induced pluripotent stem cells (hiPSCs) and in hiPSC-induced RPE cells at 30, 60, and 90 days post-differentiation, respectively. We found that LINC00167 expression was consistently upregulated along with RPE differentiation (Figure 1A). To better illustrate its role in AMD pathogenesis, we further compared its expression levels in RPE-choroid samples between AMD patients and normal controls. Clinical diagnosis and personal information of all individuals are presented in Table S1.²³ We found that LINC00167 expression was downregulated in the macular RPE-choroid tissue of AMD patients compared to normal controls (Figure 1B), but not in the extramacular tissue (Figure 1C). Our data also revealed that expression of LINC00167 was mainly reduced in the macular RPE-choroid tissue

Received 12 September 2019; accepted 29 December 2019;
<https://doi.org/10.1016/j.omtn.2019.12.040>

²These authors contribute equally to this work.

Correspondence: Qinghuai Liu, Department of Ophthalmology, The First Affiliated Hospital of Nanjing Medical University, Nanjing Medical University, Nanjing 210029, China.

E-mail: liuqh@njmu.edu.cn



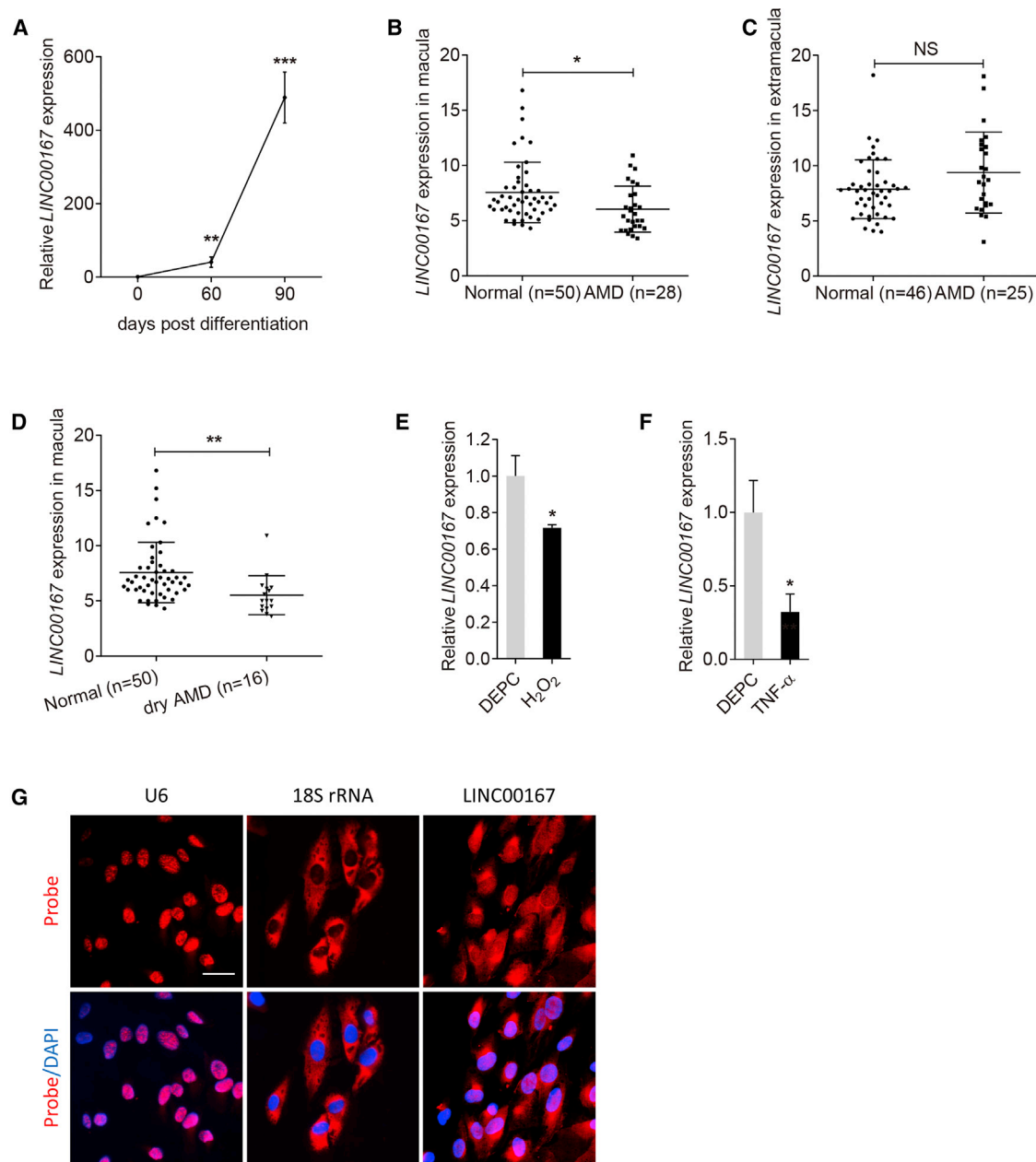
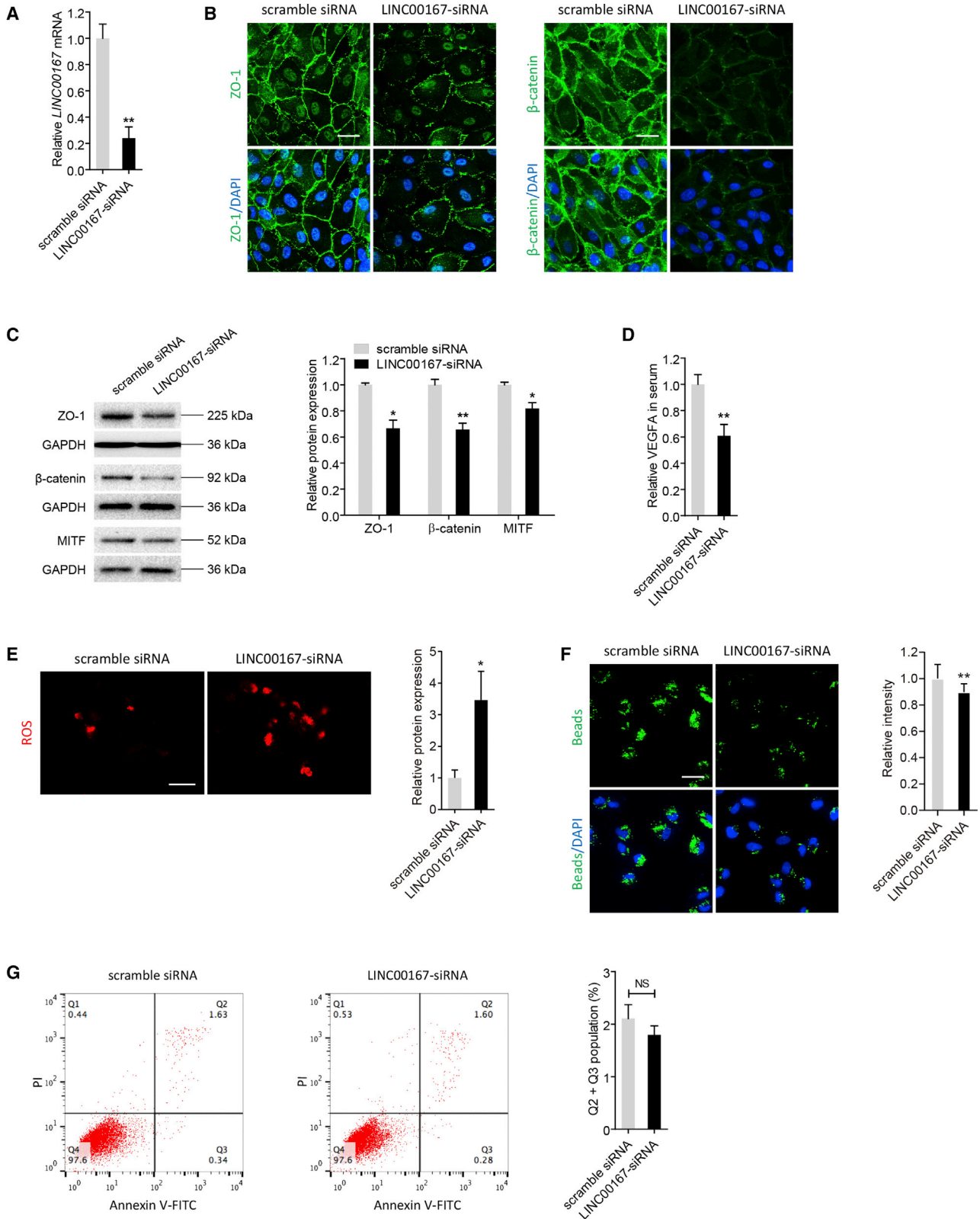


Figure 1. LINC00167 Is Decreased in AMD

(A) Expression of LINC00167 along with RPE differentiation. (B) LINC00167 expression in macular RPE-choroid tissues of normal controls and AMD patients. (C) LINC00167 expression in extramacular RPE-choroid tissues of normal controls and AMD patients. (D) LINC00167 expression in macular RPE-choroid tissues of normal controls and dry AMD patients. (E) Expression of LINC00167 in diethyl pyrocarbonate (DEPC)- and H_2O_2 -treated RPE cells. (F) Expression of LINC00167 in DEPC- and $TNF-\alpha$ -treated RPE cells. (G) Intracellular localization of U6, 18S rRNA, and LINC00167 in RPE cells as indicated by RNA-FISH. Scale bar, 20 μm . The data are presented as the mean \pm SD of three independent experiments. * $p < 0.05$, ** $p < 0.01$, *** $p < 0.001$. NS, not significant.

of dry AMD (Figure 1D). We next measured its expression pattern in dysfunctional RPE. We found that LINC00167 expression was decreased in H_2O_2 or tumor necrosis factor α ($TNF-\alpha$)-treated RPE cells (Figures 1E and 1F). Thus, our results suggested a potentially protective role of LINC00167 in AMD pathogenesis.

Function of an lncRNA mainly depends on its subcellular location. lncRNAs located in nucleus may act as neighbor gene modulators through promoter interactions, and lncRNAs expressed in cytoplasm may function as miRNA sponges.¹⁷ According to fluorescence *in situ* hybridization (FISH) results, LINC00167 was mainly located in



(legend on next page)

cytoplasm (Figure 1G), indicating its potential function as a sponge for miRNA.

LINC00167 Silencing Leads to RPE Dedifferentiation

We next tried to determine the effects of LINC00167 on RPE differentiation. Quantitative real-time PCR showed a 75% reduction of LINC00167 expression in adult RPE-19 (ARPE-19) cells transfected with LINC00167-small interfering RNA (siRNA) compared to cells transfected with scramble siRNA (Figure 2A). We then adopted immunoblotting and immunofluorescence to compare expressions of RPE characteristic markers, including tight junction protein ZO-1 (NP_003248), β -catenin (NP_001895), and microphthalmia-associated transcription factor (MITF; NP_001341533), between the LINC00167-siRNA-transfected group and the scramble siRNA-transfected group. Based on our data, endogenous LINC00167 insufficiency suppressed expressions of those markers (Figures 2B and 2C). Our findings suggested that LINC00167 promoted differentiation of RPE cells.

We next tested whether LINC00167 insufficiency would cause other forms of RPE abnormalities. Secretion of vascular endothelial growth factor A (VEGFA) is an essential function of RPE cells,⁴ which maintains the health of choriocapillaris endothelium. Insufficient VEGFA secretion is an important contributing factor for dry AMD. We therefore used an enzyme linked immunosorbent assay (ELISA) to determine VEGFA secretion of RPE cells in culture medium. A decreased amount of VEGFA was found in RPE cells with LINC00167 knocked down compared to the control group (Figure 2D). Oxidative stress, which leads to accumulation of mitochondrial reactive oxygen species (ROS), contributes to RPE dysfunction and AMD pathogenesis.^{1,5} Herein, we found that ROS generation was increased in RPE cells with LINC00167 silenced (Figure 2E). Another crucial function of RPE cells is phagocytizing photoreceptor outer segment debris, which maintains retinal homeostasis. Impaired RPE phagocytosis leads to deposition of apolipoprotein B100 and formation of drusen and basal deposits, which are important histopathologic changes in dry AMD.^{24,25} According to our results, attenuated phagocytosis was revealed in RPE cells with endogenous LINC00167 insufficiency when compared to cells transfected with scramble siRNA (Figure 2F). To rule out the possibility that such disturbed phagocytosis was caused by RPE cell death, we next measured RPE apoptosis rates in different transfected groups. No statistical difference in apoptosis rates was detected between RPE cells transfected with LINC00167-siRNA and scramble siRNA (Figure 2G). Thus, LINC00167 insufficiency impaired phagocytosis independent of RPE cell death.

Figure 2. LINC00167 Silencing Leads to RPE Dedifferentiation

(A) Relative expression of LINC00167 in ARPE-19 cells transfected with LINC00167-siRNA compared to cells transfected with scramble siRNA. (B) Expressions and intracellular localizations of RPE markers ZO-1 and β -catenin were compared between ARPE-19 cells transfected with LINC00167-siRNA and scramble RNA using immunofluorescence staining. Scale bars, 20 μ m. (C) Immunoblotting was applied to compare expression levels of ZO-1, β -catenin, and MITF between ARPE-19 cells transfected with LINC00167-siRNA and scramble RNA. A representative image and the quantification results are shown. (D) Secreted VEGFA levels in serum of ARPE-19 cells transfected with LINC00167-siRNA and scramble siRNA. (E) Mitochondrial ROS was visualized in ARPE-19 cells transfected with LINC00167-siRNA and scramble siRNA. A representative image and the quantification results are shown. Scale bar, 50 μ m. (F) Phagocytic ability was tested in ARPE-19 transfected with LINC00167-siRNA and scramble siRNA. A representative image and the quantification results are shown. Scale bar, 20 μ m. (G) Apoptosis rates were monitored by flow cytometric analysis in ARPE-19 cells transfected with LINC00167-siRNA and scramble siRNA. A representative image and the quantification results are shown. The data are presented as the mean \pm SD of three independent experiments. * p < 0.05, ** p < 0.01. NS, not significant.

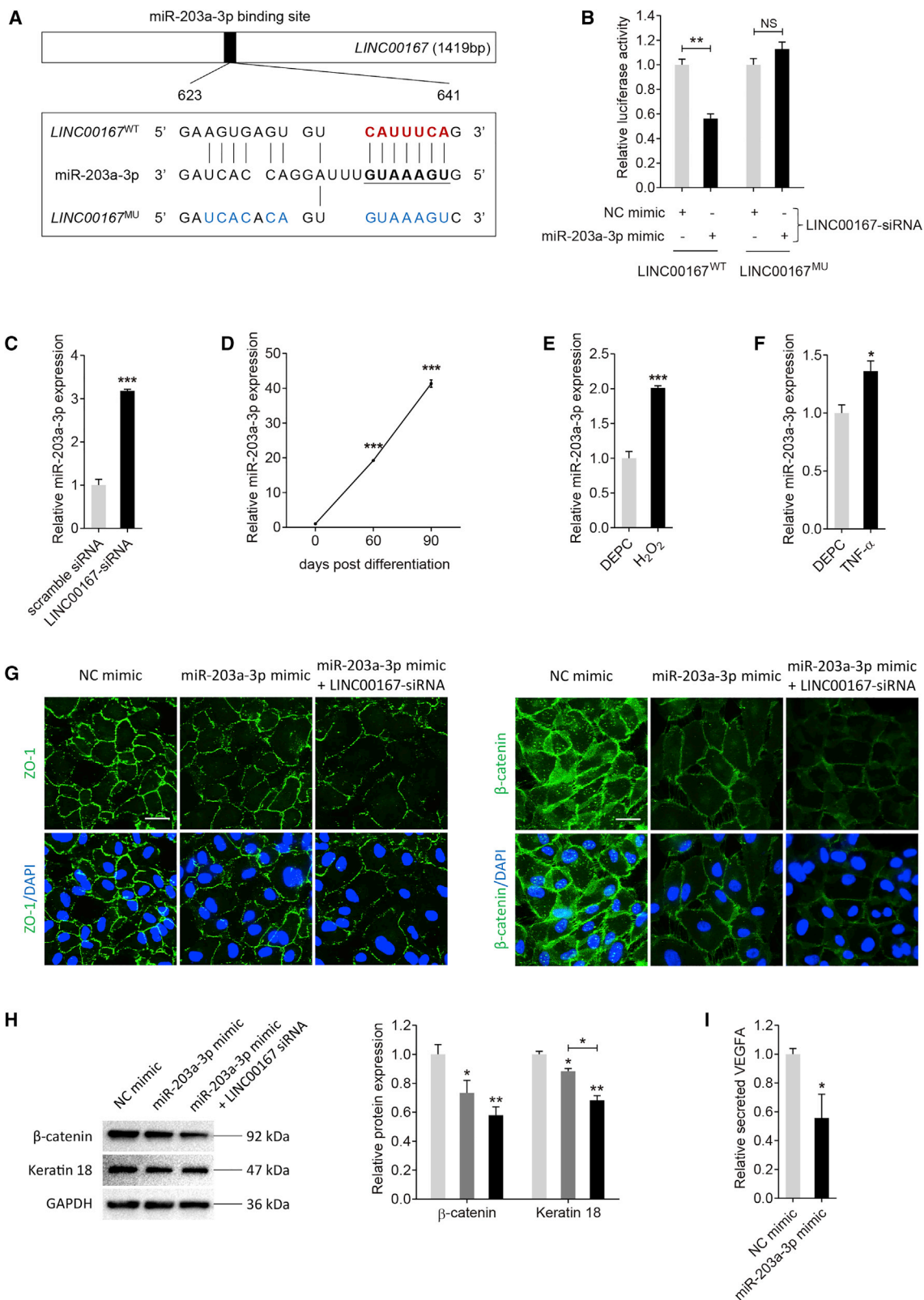
LINC00167 Functions as a Sponge for miR-203a-3p in RPE Cells

lncRNAs with miRNA-binding sites might function as miRNA sponges²⁶ and are involved in lots of biological processes and disease etiologies.²⁷ As LINC00167 was mainly localized in the cytoplasm, we hypothesized that it might act as a miRNA sponge in RPE cells. miR-203a-3p was revealed as a potential target of LINC00167 as predicted by miRcode online software (<http://mircode.org/>). We initially verified the interaction between LINC00167 and miR-203a-3p using luciferase reporter assay. LINC00167^{MU} plasmid contained 13 mutated nucleotides in the core binding region with miR-203a-3p (Figure 3A). According to our data, luciferase activity was reduced in RPE cells co-transfected with wild-type LINC00167 (LINC00167^{WT}), miR-203a-3p mimic, and LINC00167-siRNA compared to cells co-transfected with LINC00167^{WT}, negative control (NC) mimic, and LINC00167-siRNA (Figure 3B). Introduction of the mutation abolished the ability of LINC00167 to bind to miR-203a-3p (Figure 3B). We then tried to determine whether LINC00167 expression was negatively correlated with miR-203a-3p. We found that miR-203a-3p was upregulated in cells transfected with LINC00167 siRNA compared to scramble siRNA (Figure 3C). We also found that miR-203a-3p was consistently upregulated along with RPE differentiation (Figure 3D), and was increased in RPE cells treated with H₂O₂ or TNF- α (Figures 3E and 3F). Taken together, our data suggested that LINC00167 acted as a miR-203a-3p sponge in RPE cells.

The LINC00167/miR-203a-3p/SOCS3 Axis Regulates RPE Differentiation

We then analyzed the role of miR-203a-3p on RPE differentiation. According to our data, exogenous miR-203a-3p overexpression led to downregulation of RPE characteristic proteins, including ZO-1, β -catenin, and keratin 18, as revealed by immunofluorescence and immunoblotting (Figures 3G and 3H). We also found that silencing of LINC00167 and overexpression of miR-203a-3p at the same time could show double hit effects on RPE cells. Expression of RPE markers was more reduced in RPE cells transfected with both LINC00167 siRNA and miR-203a-3p mimic (Figures 3G and 3H). Our data also revealed that VEGFA secretion was disturbed in RPE cells transfected with miR-203a-3p mimic when compared to the control group (Figure 3I).

The suppressor of cytokine signaling 3 (SOCS3) gene was previously identified as a direct target of miR-203a-3p.^{28,29} SOCS3 was reported to show a protective role in AMD etiology by regulating the Janus



(legend on next page)

kinase/signal transducer and activator of transcription (JAK/STAT) cell signaling pathway.³⁰ We therefore tested whether SOCS3 was a target of miR-203a-3p in RPE cells. Expressions of both SOCS3 mRNA and protein were decreased in RPE cells transfected with miR-203a-3p mimic and increased in RPE cells transfected with miR-203a-3p inhibitor (Figures 4A and 4B), showing a reverse expressional correlation between SOCS3 and miR-203a-3p. Our data suggested that SOCS3 was negatively regulated by miR-203a-3p.

We also used gene set enrichment analysis (GSEA) to speculate on possible signaling pathways associated with LINC00167. The JAK/STAT pathway, in which SOCS3 is a key negative regulator, has a negative correlation with LINC00167 (Figure 4C). Taking all off the above findings into consideration, SOCS3 was identified as a downstream part of LINC00167/miR-203a-3p.

We next investigated its role in mediating RPE function. SOCS3 mRNA expression was consistently upregulated along with RPE differentiation (Figure 4D), and it was downregulated in H₂O₂- or TNF- α -treated RPE cells (Figures 4E and 4F). SOCS3 siRNA was applied to reduce endogenous SOCS3 expression in RPE cells (Figure S1A), and the AcFLAG-SOCS3 vector was used to overexpress SOCS3 in RPE cells (Figure S1B). According to our results, RPE characteristic proteins, including ZO-1 and β -catenin, were degraded in RPE cells transfected with SOCS3 siRNA (Figure 4G). We further aimed to tell whether miR-203a-3p regulated RPE function through SOCS3. Protein levels of ZO-1 and β -catenin were more reduced in RPE cells co-transfected with SOCS3 siRNA and miR-203a-3p when compared to cells transfected with SOCS3 siRNA alone (Figure 4G). To better tell whether SOCS3 is the downstream target of LINC00167, we tested whether overexpression of SOCS3 could rescue the LINC00167 knockdown phenotype. According to our data, overexpression of SOCS3 could rescue the negative effect of LINC00167-siRNA on RPE cells (Figure 4H). Thus, our findings indicated that the LINC00167/miR-203a-3p/SOCS3 axis participated in RPE differentiation.

DISCUSSION

RPE dedifferentiation is revealed as an initial pathological event for AMD.¹ Therefore, illustration of the mechanism underlying RPE dedifferentiation may help with the identification of therapeutic targets for AMD. lncRNAs are involved in the pathogenesis of multiple diseases, including carcinoma, neural degeneration, and cardiovascular and ocular diseases,^{16,17,21,31} while its role in AMD

etiology and RPE dedifferentiation has not been fully elucidated. We have previously found that lncRNA ZNF503-AS1 could promote RPE differentiation by downregulating ZNF503 expression.¹⁴ However, more investigations in this area are still warranted. In this study, we revealed that LINC00167 was downregulated during RPE differentiation and mediated RPE differentiation through the LINC00167/miR-203a-3p/SOCS3 axis.

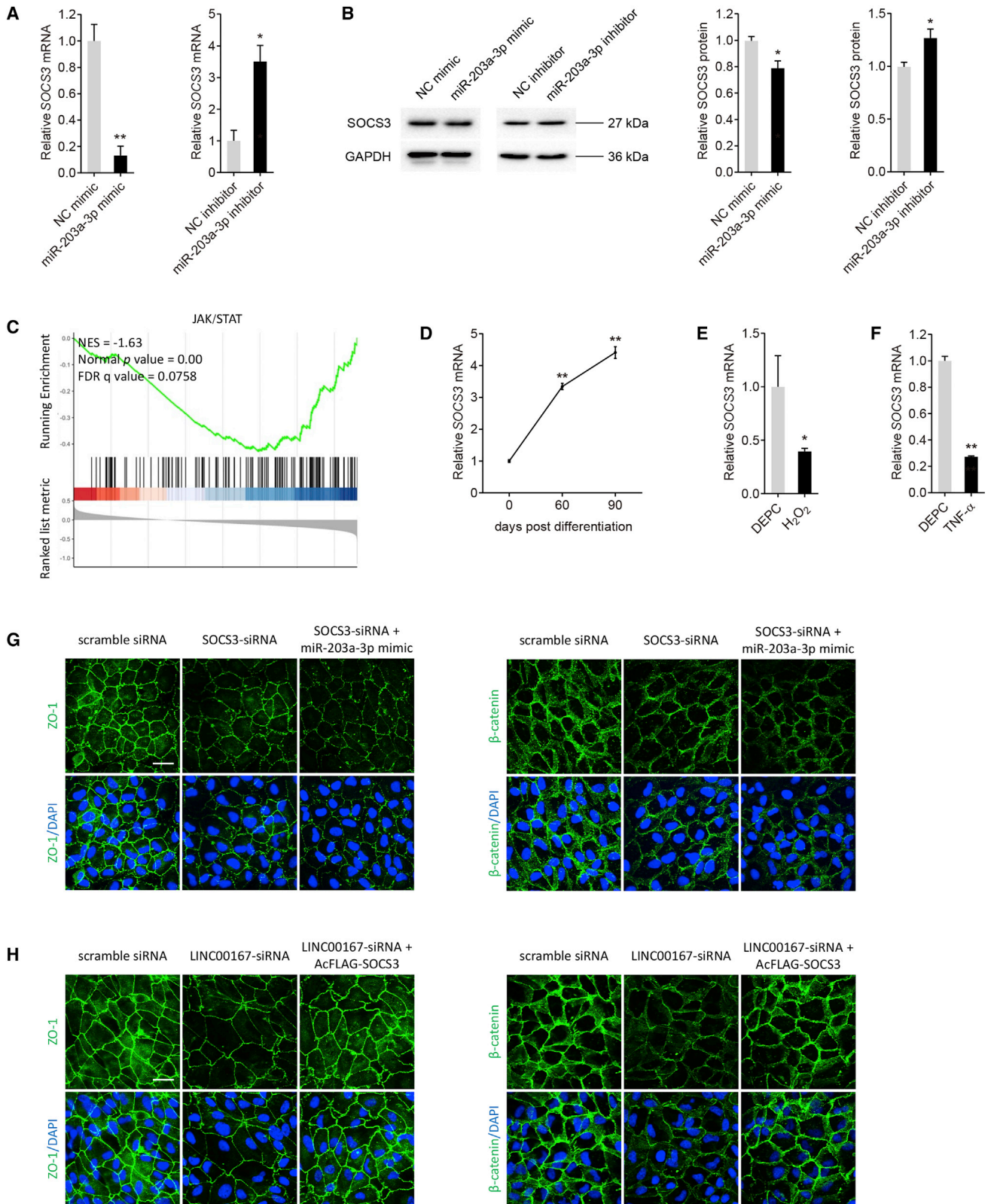
LINC00167 belongs to intergenic lncRNAs that possess an exon-intron-exon structure but do not code for proteins.³² In the present study, we found that LINC00167 expression was constantly upregulated along with RPE differentiation, and it was decreased in RPE-choroid samples of AMD patients and in H₂O₂- or TNF- α -treated RPE cells. *In vitro* study revealed that LINC00167 insufficiency led to RPE dedifferentiation, which attenuated RPE function by impairing phagocytosis, disturbing VEGFA secretion, and accelerating ROS production. As LINC00167 was found mainly localized in RPE cytoplasm, we speculated that it might function as a competitive endogenous RNA (ceRNA). ceRNAs are lncRNAs that share one or more miRNA response elements with mRNAs and function as natural pseudogenes to regulate miRNA activities.^{18,31} Involvement of lncRNA-miRNA-mRNA loops in ocular diseases have been previously revealed.^{33,34} In this study, we first revealed that LINC00167 inhibited RPE dedifferentiation and AMD progression by sponging miR-203a-3p to block its interaction with SOCS3 (Figure 5).

miRNAs are small non-coding RNAs that regulate protein production through binding to the 3' untranslated region (3' UTR) of mRNA.³⁵ miR-203a-3p has been shown to participate in diverse diseases, including cancer, ocular diseases, and cardiovascular diseases.^{29,36-38} Herein, we first revealed that overexpression of miR-203a-3p resulted in RPE dedifferentiation. A previous study revealed that miR-203a-3p was decreased in an oxygen-induced retinopathy model and mechanically repressed angiogenesis by targeting VEGFA and hypoxia-inducible factor-1 α (HIF-1 α).³⁷ miR-203a-3p was identified to specifically bind to the 3' UTR of VEGFA in human retinal microvascular endothelial cells. Similar to these findings, we also found that miR-203a-3p overexpression in RPE cells attenuated VEGFA secretion.

AMD is a comprehensive disease with both genetic and non-genetic components involved in its pathogenesis.^{39,40} Other than epigenetic regulations, other factors, such as genetic variants and

Figure 3. LINC00167 Functions as a Sponge for miR-203a-3p in RPE Cells

(A) Schematic diagram of the interaction between LINC00167 and miR-203a-3p. (B) Relative luciferase activities in ARPE-19 cells transfected with LINC00167-siRNA and LINC00167^{WT} or LINC00167^{MU} and miR-203a-3p mimic or NC mimic. (C) Relative miR-203a-3p expression in cells transfected with LINC00167-siRNA and scramble RNA. (D) Expression of miR-203a-3p along with RPE differentiation. (E) Expression of LINC00167 in diethyl pyrocarbonate (DEPC)- and H₂O₂-treated RPE cells. (F) Expression of LINC00167 in DEPC- and TNF- α -treated RPE cells. (G) RPE characteristic markers ZO-1 and β -catenin were observed by immunofluorescence staining in ARPE-19 cells transfected with NC mimic, miR-203a-3p mimic, and miR-203a-3p mimic together with LINC00167-siRNA. Scale bars, 20 μ m. (H) Expression levels of RPE markers β -catenin and keratin 18 were monitored by immunoblotting in ARPE-19 cells transfected with NC mimic, miR-203a-3p mimic, and miR-203a-3p mimic together with LINC00167-siRNA. (I) Secreted VEGFA levels in serum of ARPE-19 cells transfected with NC mimic and miR-203a-3p mimic. The data are presented as the mean \pm SD of three independent experiments. *p < 0.05, **p < 0.01, ***p < 0.001. NS, not significant.



(legend on next page)

environmental variables, have also been found to be associated with AMD susceptibility. Of note, polymorphisms within precursor (pre)-miRNA sequences have been reported to contribute to AMD etiology.^{41,42} Such polymorphisms might affect the functional activities of miRNAs, especially the interaction of miRNAs with specific targets. Multivariate risk indexes might cooperate together to alter signaling pathways such as complement activation, inflammation, VEGFA signaling, and oxidative stress,⁴⁰ and further contribute to the pathogenesis of AMD. The pharmacogenetic relationship between genetic variants and the variable response of AMD patients to anti-VEGF therapies has been widely investigated.⁴³ Due to the regulatory role of miR-203a-3p on VEGFA expression, genetic variants in the LINC00167/miR-203a-3p axis might also function as a pharmacoeigenetic biomarker for AMD patients to determine the dosage and administration frequency of anti-VEGF drugs.

We also identified SOCS3 as a direct target of miR-203a-3p in RPE cells. SOCS3 has been revealed as an inhibitor of the JAK/STAT pathway in various studies.^{30,44–52} SOCS3 was previously reported to show a protective effect on AMD pathogenesis by regulating the JAK/STAT pathway.³⁰ A recent study also revealed that SOCS3 deficiency promoted inflammation-related retinal degeneration in experimental autoimmune uveoretinitis mice.⁵³ In mammals, the JAK/STAT signaling pathway is reported to participate in various biological processes, including inflammation, cell differentiation, proliferation, migration, and apoptosis.⁵⁴ Previous studies have identified an inhibitory role of the JAK/STAT pathway in cell differentiation. Activation of the JAK/STAT pathway reversed differentiated spermatogonia into stem cell-like status.⁴⁸ Partial inhibition of the JAK/STAT pathway by SOCS3 disturbed dedifferentiation of spermatogonia into germline stem cells in *Drosophila* testis.⁵¹ Herein, our study demonstrated that oxidative stress and inflammation downregulated SOCS3 expression in RPE cells. We also revealed that SOCS3 was regulated by the LINC00167/miR-203a-3p axis and mediated RPE dedifferentiation by repressing the JAK/STAT pathway. Therefore, JAK/STAT inhibitors show promising prospects in AMD treatment. However, LINC00167 might have other sponging miRNAs besides miR-203a-3p, and the LINC00167/miR-203a-3p axis might regulate RPE function through other pathways in addition to the SOCS3/JAK/STAT pathway. Thus, more investigations are warranted to better elucidate the regulatory network of LINC00167 in RPE cells. Another limitation of this study is the lack of patient samples to verify the downstream regulatory network of LINC00167 in patients. We will keep working on that in our future studies.

In conclusion, our study revealed that LINC00167 inhibited RPE dedifferentiation and AMD progression by sponging miR-203a-3p to block its interaction with SOCS3. Thus, LINC00167 might be a potential therapeutic target for AMD.

MATERIALS AND METHODS

Samples

Sample information and microarray data (GEO: GSE29801) of 78 independent macular and 71 extramacular RPE-choroid samples were downloaded from Gene Expression Omnibus datasets and analyzed as described previously.²³ Information of all samples and their LINC00167 expression levels are detailed in [Table S1](#).

Cell Culture, Treatment, and Transfection

hiPSCs (IMR90-57) were grown on mouse embryonic fibroblasts (SiDan-Sai Biotechnology, Shanghai, China) in a six-well plate as described before.⁵⁵ *In vitro* differentiation of hiPSCs to RPE cells was conducted using the SFEB/CS method. CKI-7 (5 μ M) and SB-431542 (5 μ M) were added to trigger differentiation. ARPE-19 cells purchased from American Type Culture Collection were cultured in Dulbecco's modified Eagle's/F12 medium supplemented with 10% fetal bovine serum (Gibco, Grand Island, NY, USA) and 1% penicillin/streptomycin. Cells were incubated at 37°C in 5% CO₂. For the H₂O₂ assay, ARPE-19 cells were incubated with H₂O₂ at the concentration of 200 μ M for 48 h before collection. For the TNF- α assay, cells were treated with TNF- α at the concentration of 100 ng/mL for 48 h before collection. For the transfection assay, cells were seeded into six-well templates and transfected with 100 pmol of siRNA/mimic/inhibitor and/or 4 μ g of plasmid, using Lipofectamine 3000 transfection reagent (Invitrogen, Carlsbad, CA, USA) per well according to the manufacturer's protocol. NC mimic and inhibitor, miR-203a-3p mimic and inhibitor (2'-O-methyl modification), scramble siRNA, LINC00167-siRNA, and SOCS3-siRNA were purchased from RiboBio (Guangzhou, China) with sequences detailed in [Table S2](#). The open reading frame sequence of SOCS3 was synthesized and inserted into pCMV-C-FLAG plasmid (Beyotime, Shanghai, China) to produce the recombinant plasmid AcFLAG-SOCS3. Cells were collected at 48 h post-transfection for RNA extraction, and at 72 h post-transfection for immunoblotting, immunofluorescence staining, apoptosis analysis, ROS measurement, and luciferase reporter assay.

RNA Extraction, Reverse Transcriptase PCR (RT-PCR), and Quantitative Real-Time PCR

Total RNA was extracted using TRIzol reagent (Invitrogen) according to the manufacturer's instructions. A NanoDrop ND-1000

Figure 4. miR-203a-3p/SOCS3 Axis Regulates RPE Differentiation

(A and B) Relative expression of SOCS3 mRNA (A) and protein (B) in ARPE-19 cells transfected with NC mimic, miR-203a-3p mimic, NC inhibitor, and miR-203a-3p inhibitor. (C) JAK/STAT enrichment analysis. (D) Expression of SOCS3 along with RPE differentiation. (E) Expression of SOCS3 in diethyl pyrocarbonate (DEPC)- and H₂O₂-treated RPE cells. (F) Expression of SOCS3 in DEPC- and TNF- α -treated RPE cells. (G) We used immunofluorescence staining to visualize RPE characteristic markers ZO-1 and β -catenin in ARPE-19 cells transfected with scramble siRNA, SOCS3-siRNA, and SOCS3-siRNA together with miR-203a-3p mimic. Scale bar, 20 μ m. (H) Immunofluorescence staining was applied to compare expressions of ZO-1 and β -catenin in ARPE-19 cells transfected with scramble siRNA, LINC00167-siRNA, and LINC00167-siRNA together with AcFLAG-SOCS3. Scale bar, 20 μ m. The data are presented as the mean \pm SD of three independent experiments. *p < 0.05, **p < 0.01, ***p < 0.001.

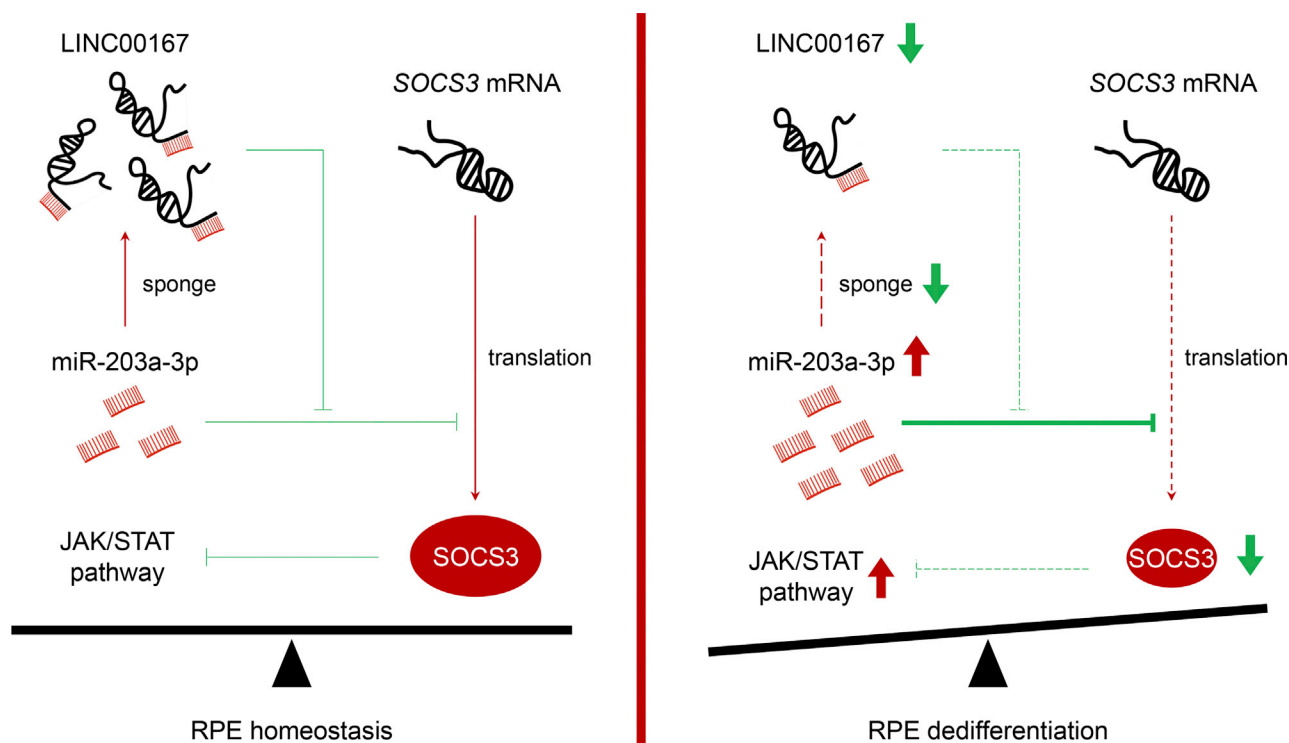


Figure 5. Schematic Illustration of the LINC00167/miR-203a-3p/SOCS3 Axis in Normal RPE Cells and Dedifferentiated RPE Cells

miR-203a-3p binds to both LINC00167 and the 3' UTR of SOCS3. When expression of LINC00167 is downregulated, an increased amount of miR-203a-3p would bind to the SOCS3 3' UTR to decrease SOCS3 protein expression in a post-transcriptional way. This would lead to RPE dedifferentiation.

spectrophotometer (NanoDrop Technologies, Wilmington, DE, USA) was used to detect concentration and quality of RNA samples. 1 μ g of total RNA was used for RT-PCR using a PrimeScript RT kit (Takara, Otsu, Shiga, Japan). Quantitative real-time PCR was conducted using FastStart Universal SYBR Green Master (Rox; Roche, Basel, Switzerland) with the StepOne Plus real-time PCR system (Applied Biosystems, Darmstadt, Germany). Primers used in this study were *LINC00167* (forward, 5'-TCAGTCACTCC TTAACCGC-3'; reverse, 5'-TCTCTCTGCCATCTAGCTGC-3'), 18S ribosomal RNA (18S rRNA; forward, 5'-TTAATTCGATAA CGAACGAGA-3'; reverse, 5'-CGCTGAGCCAGTCAGTGTAG-3'), *SOCS3* (forward, 5'-CACTCTCCAGCATCTCTGTC-3'; reverse, 5'-TCGTA CTGTTCCAGGA ACTC-3'), *GAPDH* (forward, 5'-CAG CCTCAAGATCATCAGCA-3'; reverse, 5'-TGTGGTCATGAGT CCTTCCA-3'). Bulge-loop miRNA RT-PCR primer sets (one RT primer and a pair of quantitative real-time PCR primers for each set) were designed by RiboBio.

FISH

LINC00167, U6, and 18S rRNA FISH probes were purchased from RiboBio. FISH was conducted according to the manufacturer's protocol (RiboBio). ARPE-19 cells were seeded into a 12-well plate, fixed with 4% paraformaldehyde (PFA), permeabilized in 0.5% Triton X-100 for 10 min on ice, and then covered with pre-hybridization buffer. After removal of pre-hybridization buffer, cells were hybrid-

ized with a Cy3-labeled LINC00167 probe and placed in a 37°C incubator overnight. Cell nuclei were counterstained by 4',6-diamidino-2-phenylindole (DAPI). Images were taken with a confocal microscope (LSM 510; Carl Zeiss, Jena, Germany).

Immunofluorescence Staining

Cells were fixed with 4% PFA, permeabilized with 0.5% Triton X-100, blocked in 5% bovine serum albumin, and incubated in primary antibody reagents at 4°C overnight. Details for antibodies are provided in Table S3. Cells were then washed with phosphate-buffered saline (PBS) three times and incubated in corresponding fluorescence-conjugated secondary antibodies (1:1,000 diluted in 1 \times PBS; Invitrogen) for 1 h at room temperature. Cell nuclei were stained by DAPI (Sigma, St. Louis, MO, USA). Images were collected by a confocal microscope (LSM 510).

Immunoblotting

Extracted protein was separated by 10% sodium dodecyl sulfate polyacrylamide gel electrophoresis and transferred to a polyvinylidene fluoride membrane (Millipore, Billerica, MA, USA). Membranes were blocked in 5% skim milk at 37°C for 1 h and incubated with primary antibody reagents at 4°C overnight. Details for antibodies are provided in Table S3. After incubation, membranes were washed with Tris-buffered saline with Tween 20 (TBST) and probed with corresponding horseradish peroxidase-conjugated secondary antibodies

(1:5,000 diluted in TBST; ICL, Newberg, OR, USA) for 2 h at room temperature. Blots were then developed by autoradiography with the enhanced chemiluminescence (ECL)-western blotting system (Bio-Rad, Hercules, CA, USA) following the manufacturer's protocol. ImageJ software (<https://imagej.nih.gov/ij/index.html>) was utilized to measure protein intensities.

Mitochondrial ROS Measurement

ARPE-19 cells were grown on 12-well plates. Mitochondrial ROS were detected using the MitoSOX Red mitochondrial superoxide indicator (Invitrogen) according to the manufacturer's protocol. Cells were treated with 5 μ M MitoSOX probe at 37°C for 10 min. A Leica DM4000 B LED microscope (Leica, Wetzlar, Germany) was used to detect ROS signal.

Analyses of Phagocytosis

Phagocytic ability was conducted according to a previously described protocol.³ Briefly, ARPE-19 cells were planted on eight-well chamber slides (Millipore, Billerica, MA, USA) and harvested at 72 h post-transfection. Cells were then incubated with carboxylate-modified polystyrene latex beads (diameter, 1 μ m; emission maximum, 515 nm; Sigma) at 37°C for 12 h, washed with 1 \times PBS, and then treated with 0.2% trypan blue to quench extracellular fluorescence. Cell nuclei were counterstained with DAPI. An LSM 510 confocal microscope was applied for image collection. We used ImageJ software to quantify fluorescence.

Apoptosis Analysis

ARPE-19 cells were harvested and incubated with annexin V-fluorescein isothiocyanate (FITC; Vazyme, Nanjing, China) and propidium iodide (Vazyme) according to the manufacturer's protocol. Flow cytometric analysis was then performed to examine apoptotic cells using a Gallios flow cytometry (Beckman Coulter, Brea, CA, USA). A total of 10,000 living cells were collected for examination. Data were plotted and analyzed using FlowJo v10 software. Annexin V-FITC-positive cells were considered as apoptotic cells.

Luciferase Reporter Assay

The luciferase reporter assay was conducted according to a previously described protocol.¹⁴ The entire LINC00167 sequence was synthesized and inserted into the pGL3-promoter vector (Promega, Madison, WI, USA) using the *Xba*I restriction site to generate the recombinant plasmids LINC00167^{WT} and LINC00167^{MU}. The LINC00167^{MU} contained seven mutated nucleotides in the core binding region with miR-203a-3p. Constructed plasmids were sequenced and confirmed with Sanger sequencing. ARPE-19 cells were seeded into 24-well plates and transfected with 16 ng of cytomegalovirus-Renilla (Promega), 20 pmol of miR-203a-3p mimic or NC mimic, and 800 ng of LINC00167^{WT} or LINC00167^{MU} per well using Lipofectamine 3000 transfection reagent (Invitrogen). Luciferase activities were measured by a dual-luciferase system (Promega) using a GloMax-96 luminometer. Renilla luciferase activities were used as internal standard indicators for transfection efficiency. Firefly luciferase activities were then normalized to Renilla luciferase activities.

ELISA

ARPE-19 cells were grown on a six-well plate with culture medium and were collected at 72 h post-transfection for ELISA. The expression level of VEGFA was determined using a commercial human VEGFA ELISA kit (Beijing 4A Biotech, Beijing, China) according to the manufacturer's protocol.

Bioinformatics Analysis

GSEA (<http://software.broadinstitute.org/gsea/msigdb/index.jsp>) was used to identify enriched gene sets in the Kyoto Encyclopedia of Genes and Genomes based on the Pearson's correlation coefficient with LINC00167 and expression profile of mRNAs in previous study was used as input.²³ GraphPad Prism (version 8.0; GraphPad, San Diego, CA, USA) was used for statistical analysis. One-way analysis of variance and a two-tailed Student's *t* test were used for comparisons between different groups. All experiments were performed in triplicate, with data being averaged. A *p* value <0.05 was considered as statistically significant.

SUPPLEMENTAL INFORMATION

Supplemental Information can be found online at <https://doi.org/10.1016/j.omtn.2019.12.040>.

AUTHOR CONTRIBUTIONS

X.C. and Q.L. conceived and designed the study. X.C. and R.S. conducted experiments, analyzed data, and drafted the manuscript. Q.L. interpreted the data and revised the manuscript. D.Y. and C.J. coordinated and analyzed the data. All the authors contributed to, read, and approved the final manuscript.

CONFLICTS OF INTEREST

The authors declare no competing interests.

ACKNOWLEDGMENTS

This study was supported by the National Natural Science Foundation of China (81770973 to Q.L. and 81700877 to X.C.); the National Key Research and Development Program of China (2017YFA0104100 to Q.L.); the Natural Science Foundation of Jiangsu Province (BK20171087 to X.C.); the Six Talent Peaks Project in Jiangsu Province (WSW-004 to X.C.); and a project funded by the Priority Academic Program Development (PAPD) of Jiangsu Higher Education Institutions.

REFERENCES

- Zhao, C., Yasumura, D., Li, X., Matthes, M., Lloyd, M., Nielsen, G., Ahern, K., Snyder, M., Bok, D., Dunaief, J.L., et al. (2011). mTOR-mediated dedifferentiation of the retinal pigment epithelium initiates photoreceptor degeneration in mice. *J. Clin. Invest.* 121, 369–383.
- Strauss, O. (2005). The retinal pigment epithelium in visual function. *Physiol. Rev.* 85, 845–881.
- Jiang, C., Xie, P., Sun, R., Sun, X., Liu, G., Ding, S., Zhu, M., Yan, B., Liu, Q., Chen, X., and Zhao, C. (2018). c-Jun-mediated microRNA-302d-3p induces RPE dedifferentiation by targeting p21^{Waf1/Cip1}. *Cell Death Dis.* 9, 451.

4. Saint-Geniez, M., Kurihara, T., Sekiyama, E., Maldonado, A.E., and D'Amore, P.A. (2009). An essential role for RPE-derived soluble VEGF in the maintenance of the choriocapillaris. *Proc. Natl. Acad. Sci. USA* *106*, 18751–18756.
5. Datta, S., Cano, M., Ebrahimi, K., Wang, L., and Handa, J.T. (2017). The impact of oxidative stress and inflammation on RPE degeneration in non-neovascular AMD. *Prog. Retin. Eye Res.* *60*, 201–218.
6. van Lookeren Campagne, M., LeCouter, J., Yaspan, B.L., and Ye, W. (2014). Mechanisms of age-related macular degeneration and therapeutic opportunities. *J. Pathol.* *232*, 151–164.
7. Gehrs, K.M., Anderson, D.H., Johnson, L.V., and Hageman, G.S. (2006). Age-related macular degeneration—emerging pathogenetic and therapeutic concepts. *Ann. Med.* *38*, 450–471.
8. Bressler, N.M. (2004). Age-related macular degeneration is the leading cause of blindness. *JAMA* *291*, 1900–1901.
9. Augustin, A., Sahel, J.A., Bandello, F., Dardennes, R., Maurel, F., Negrini, C., Hieke, K., and Berdeaux, G. (2007). Anxiety and depression prevalence rates in age-related macular degeneration. *Invest. Ophthalmol. Vis. Sci.* *48*, 1498–1503.
10. Wong, W.L., Su, X., Li, X., Cheung, C.M., Klein, R., Cheng, C.Y., and Wong, T.Y. (2014). Global prevalence of age-related macular degeneration and disease burden projection for 2020 and 2040: a systematic review and meta-analysis. *Lancet Glob. Health* *2*, e106–e116.
11. Mitchell, P., Liew, G., Gopinath, B., and Wong, T.Y. (2018). Age-related macular degeneration. *Lancet* *392*, 1147–1159.
12. Li, W. (2013). Phagocyte dysfunction, tissue aging and degeneration. *Ageing Res. Rev.* *12*, 1005–1012.
13. Ach, T., Tolstik, E., Messinger, J.D., Zarubina, A.V., Heintzmann, R., and Curcio, C.A. (2015). Lipofuscin redistribution and loss accompanied by cytoskeletal stress in retinal pigment epithelium of eyes with age-related macular degeneration. *Invest. Ophthalmol. Vis. Sci.* *56*, 3242–3252.
14. Chen, X., Jiang, C., Qin, B., Liu, G., Ji, J., Sun, X., Xu, M., Ding, S., Zhu, M., Huang, G., et al. (2017). lncRNA *ZNF503-AS1* promotes RPE differentiation by downregulating *ZNF503* expression. *Cell Death Dis.* *8*, e3046.
15. Sulzbacher, F., Kiss, C., Kaider, A., Eisenkoelbl, S., Munk, M., Roberts, P., Sacu, S., and Schmidt-Erfurth, U. (2012). Correlation of SD-OCT features and retinal sensitivity in neovascular age-related macular degeneration. *Invest. Ophthalmol. Vis. Sci.* *53*, 6448–6455.
16. Li, F., Wen, X., Zhang, H., and Fan, X. (2016). Novel insights into the role of long non-coding RNA in ocular diseases. *Int. J. Mol. Sci.* *17*, 478.
17. Li, X., Wu, Z., Fu, X., and Han, W. (2014). lncRNAs: insights into their function and mechanics in underlying disorders. *Mutat. Res. Rev. Mutat. Res.* *762*, 1–21.
18. Salmena, L., Poliseno, L., Tay, Y., Kats, L., and Pandolfi, P.P. (2011). A ceRNA hypothesis: the Rosetta Stone of a hidden RNA language? *Cell* *146*, 353–358.
19. Sen, R., Ghosal, S., Das, S., Balti, S., and Chakrabarti, J. (2014). Competing endogenous RNA: the key to posttranscriptional regulation. *ScientificWorldJournal* *2014*, 896206.
20. Wapinski, O., and Chang, H.Y. (2011). Long noncoding RNAs and human disease. *Trends Cell Biol.* *21*, 354–361.
21. Guttman, M., Donaghey, J., Carey, B.W., Garber, M., Grenier, J.K., Munson, G., Young, G., Lucas, A.B., Ach, R., Bruhn, L., et al. (2011). lincRNAs act in the circuitry controlling pluripotency and differentiation. *Nature* *477*, 295–300.
22. Mercer, T.R., Dinger, M.E., and Mattick, J.S. (2009). Long non-coding RNAs: insights into functions. *Nat. Rev. Genet.* *10*, 155–159.
23. Newman, A.M., Gallo, N.B., Hancox, L.S., Miller, N.J., Radeke, C.M., Maloney, M.A., Cooper, J.B., Hageman, G.S., Anderson, D.H., Johnson, L.V., and Radeke, M.J. (2012). Systems-level analysis of age-related macular degeneration reveals global biomarkers and phenotype-specific functional networks. *Genome Med.* *4*, 16.
24. Curcio, C.A., Presley, J.B., Malek, G., Medeiros, N.E., Avery, D.V., and Kruth, H.S. (2005). Esterified and unesterified cholesterol in drusen and basal deposits of eyes with age-related maculopathy. *Exp. Eye Res.* *81*, 731–741.
25. Curcio, C.A., Johnson, M., Huang, J.D., and Rudolf, M. (2009). Aging, age-related macular degeneration, and the response-to-retention of apolipoprotein B-containing lipoproteins. *Prog. Retin. Eye Res.* *28*, 393–422.
26. Paraskevopoulou, M.D., and Hatzigeorgiou, A.G. (2016). Analyzing miRNA-lncRNA interactions. *Methods Mol. Biol.* *1402*, 271–286.
27. Ballantyne, M.D., McDonald, R.A., and Baker, A.H. (2016). lncRNA/microRNA interactions in the vasculature. *Clin. Pharmacol. Ther.* *99*, 494–501.
28. Xu, J.Z., Shao, C.C., Wang, X.J., Zhao, X., Chen, J.Q., Ouyang, Y.X., Feng, J., Zhang, F., Huang, W.H., Ying, Q., et al. (2019). circTADA2As suppress breast cancer progression and metastasis via targeting miR-203a-3p/SOCS3 axis. *Cell Death Dis.* *10*, 175.
29. Muhammad, N., Bhattacharya, S., Steele, R., and Ray, R.B. (2016). Anti-miR-203 suppresses ER-positive breast cancer growth and stemness by targeting SOCS3. *Oncotarget* *7*, 58595–58605.
30. Chen, M., Lechner, J., Zhao, J., Toth, L., Hogg, R., Silvestri, G., Kissenpfennig, A., Chakravarthy, U., and Xu, H. (2016). STAT3 activation in circulating monocytes contributes to neovascular age-related macular degeneration. *Curr. Mol. Med.* *16*, 412–423.
31. Cesana, M., Cacchiarelli, D., Legnini, I., Santini, T., Sthandier, O., Chinappi, M., Tramontano, A., and Bozzoni, I. (2011). A long noncoding RNA controls muscle differentiation by functioning as a competing endogenous RNA. *Cell* *147*, 358–369.
32. Ulitsky, I., and Bartel, D.P. (2013). lincRNAs: genomics, evolution, and mechanisms. *Cell* *154*, 26–46.
33. Yan, B., Yao, J., Liu, J.Y., Li, X.M., Wang, X.Q., Li, Y.J., Tao, Z.F., Song, Y.C., Chen, Q., and Jiang, Q. (2015). lncRNA-MIAT regulates microvascular dysfunction by functioning as a competing endogenous RNA. *Circ. Res.* *116*, 1143–1156.
34. Shen, Y., Dong, L.F., Zhou, R.M., Yao, J., Song, Y.C., Yang, H., Jiang, Q., and Yan, B. (2016). Role of long non-coding RNA MIAT in proliferation, apoptosis and migration of lens epithelial cells: a clinical and in vitro study. *J. Cell. Mol. Med.* *20*, 537–548.
35. Jonas, S., and Izaurralde, E. (2015). Towards a molecular understanding of microRNA-mediated gene silencing. *Nat. Rev. Genet.* *16*, 421–433.
36. Zhang, J.J., Liu, W.Q., Peng, J.J., Ma, Q.L., Peng, J., and Luo, X.J. (2017). miR-21-5p/203a-3p promote ox-LDL-induced endothelial cell senescence through down-regulation of mitochondrial fission protein Drp1. *Mech. Ageing Dev.* *164*, 8–19.
37. Han, N., Xu, H., Yu, N., Wu, Y., and Yu, L. (2020). miR-203a-3p inhibits retinal angiogenesis and alleviates proliferative diabetic retinopathy in oxygen-induced retinopathy (OIR) rat model via targeting VEGFA and HIF-1 α . *Clin. Exp. Pharmacol. Physiol.* *47*, 85–94.
38. Chen, L., Gao, H., Liang, J., Qiao, J., Duan, J., Shi, H., Zhen, T., Li, H., Zhang, F., Zhu, Z., and Han, A. (2018). miR-203a-3p promotes colorectal cancer proliferation and migration by targeting PDE4D. *Am. J. Cancer Res.* *8*, 2387–2401.
39. Fritsche, L.G., Igl, W., Bailey, J.N., Grassmann, F., Sengupta, S., Bragg-Gresham, J.L., Burdon, K.P., Hebbaring, S.J., Wen, C., Gorski, M., et al. (2016). A large genome-wide association study of age-related macular degeneration highlights contributions of rare and common variants. *Nat. Genet.* *48*, 134–143.
40. Cascella, R., Strafella, C., Longo, G., Ragazzo, M., Manzo, L., De Felici, C., Errichiello, V., Caputo, V., Viola, F., Eandi, C.M., et al. (2017). Uncovering genetic and non-genetic biomarkers specific for exudative age-related macular degeneration: significant association of twelve variants. *Oncotarget* *9*, 7812–7821.
41. Ghanbari, M., Erkeland, S.J., Xu, L., Colijn, J.M., Franco, O.H., Dehghan, A., Klaver, C.C.W., and Meester-Smoor, M.A. (2017). Genetic variants in microRNAs and their binding sites within gene 3'UTRs associate with susceptibility to age-related macular degeneration. *Hum. Mutat.* *38*, 827–838.
42. Strafella, C., Errichiello, V., Caputo, V., Aloe, G., Ricci, F., Cusumano, A., Novelli, G., Giardina, E., and Cascella, R. (2019). The interplay between miRNA-related variants and age-related macular degeneration: evidence of association of *MIR146A* and *MIR27A*. *Int. J. Mol. Sci.* *20*, E1578.
43. Cascella, R., Strafella, C., Caputo, V., Errichiello, V., Zampatti, S., Milano, F., Potenza, S., Mauriello, S., Novelli, G., Ricci, F., et al. (2018). Towards the application of precision medicine in age-related macular degeneration. *Prog. Retin. Eye Res.* *63*, 132–146.
44. Eid, R.A., Alkhatib, M.A., Eleawa, S., Al-Hashem, F.H., Al-Shraim, M., El-Kott, A.F., Zaki, M.S.A., Dallak, M.A., and Aldera, H. (2018). Cardioprotective effect of ghrelin

- against myocardial infarction-induced left ventricular injury via inhibition of SOCS3 and activation of JAK2/STAT3 signaling. *Basic Res. Cardiol.* *113*, 13.
45. Steyn, P.J., Dzobo, K., Smith, R.L., and Myburgh, K.H. (2019). Interleukin-6 induces myogenic differentiation via JAK2-STAT3 signaling in mouse C2C12 myoblast cell line and primary human myoblasts. *Int. J. Mol. Sci.* *20*, E5273.
 46. Wonganan, O., He, Y.J., Shen, X.F., Wongkrajang, K., Suksamrarn, A., Zhang, G.L., and Wang, F. (2017). 6-Hydroxy-3-O-methyl-kaempferol 6-O-glucopyranoside potentiates the anti-proliferative effect of interferon α/β by promoting activation of the JAK/STAT signaling by inhibiting SOCS3 in hepatocellular carcinoma cells. *Toxicol. Appl. Pharmacol.* *336*, 31–39.
 47. Liu, K., Wu, Z., Chu, J., Yang, L., and Wang, N. (2019). Promoter methylation and expression of SOCS3 affect the clinical outcome of pediatric acute lymphoblastic leukemia by JAK/STAT pathway. *Biomed. Pharmacother.* *115*, 108913.
 48. Brawley, C., and Matunis, E. (2004). Regeneration of male germline stem cells by spermatogonial dedifferentiation in vivo. *Science* *304*, 1331–1334.
 49. Xu, C.H., Liu, Y., Xiao, L.M., Chen, L.K., Zheng, S.Y., Zeng, E.M., Li, D.H., and Li, Y.P. (2019). Silencing microRNA-221/222 cluster suppresses glioblastoma angiogenesis by suppressor of cytokine signaling-3-dependent JAK/STAT pathway. *J. Cell. Physiol.* *234*, 22272–22284.
 50. Croker, B.A., Kiu, H., and Nicholson, S.E. (2008). SOCS regulation of the JAK/STAT signalling pathway. *Semin. Cell Dev. Biol.* *19*, 414–422.
 51. Sheng, X.R., Brawley, C.M., and Matunis, E.L. (2009). Dedifferentiating spermatogonia outcompete somatic stem cells for niche occupancy in the *Drosophila* testis. *Cell Stem Cell* *5*, 191–203.
 52. Alexander, W.S., and Hilton, D.J. (2004). The role of suppressors of cytokine signaling (SOCS) proteins in regulation of the immune response. *Annu. Rev. Immunol.* *22*, 503–529.
 53. Chen, M., Zhao, J., Ali, I.H.A., Marry, S., Augustine, J., Bhuckory, M., Lynch, A., Kissenpfennig, A., and Xu, H. (2018). Cytokine signaling protein 3 deficiency in myeloid cells promotes retinal degeneration and angiogenesis through arginase-1 up-regulation in experimental autoimmune uveoretinitis. *Am. J. Pathol.* *188*, 1007–1020.
 54. Rawlings, J.S., Rosler, K.M., and Harrison, D.A. (2004). The JAK/STAT signaling pathway. *J. Cell Sci.* *117*, 1281–1283.
 55. Jiang, C., Qin, B., Liu, G., Sun, X., Shi, H., Ding, S., Liu, Y., Zhu, M., Chen, X., and Zhao, C. (2016). MicroRNA-184 promotes differentiation of the retinal pigment epithelium by targeting the AKT2/mTOR signaling pathway. *Oncotarget* *7*, 52340–52353.

OMTN, Volume 19

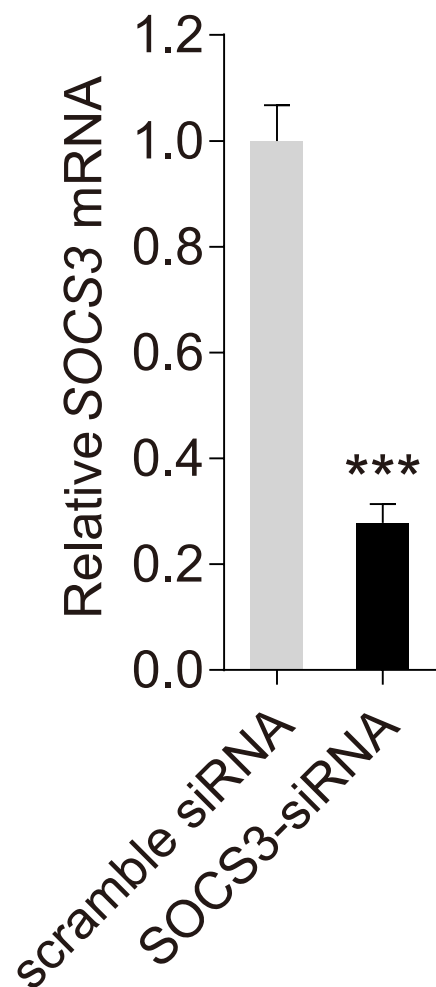
Supplemental Information

LINC00167 Regulates RPE Differentiation by Targeting the miR-203a-3p/SOCS3 Axis

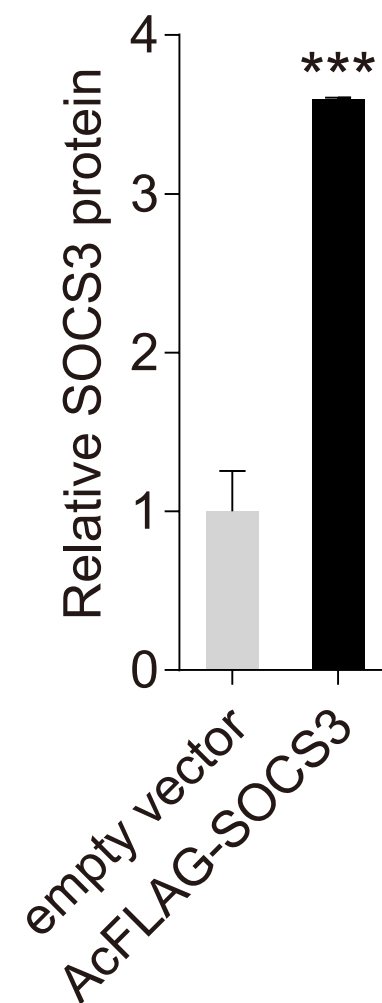
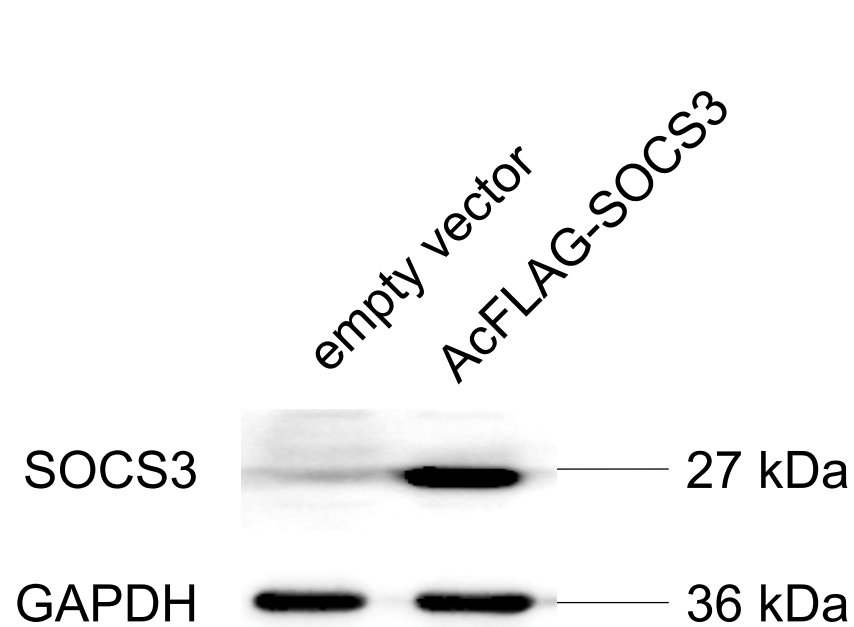
Xue Chen, Ruxu Sun, Daidi Yang, Chao Jiang, and Qinghui Liu

Supplementary Figure S1

A



B



Legend to Supplementary Figure S1

Supplementary Figure S1. Expression of SOCS3 in ARPE-19 cells transfected with siRNA or AcFLAG-SOCS3.

(A) Relative mRNA expression levels of SOCS3 in ARPE-19 cells transfected with SOCS3-siRNA or scramble siRNA. (B) Relative protein expression of SOCS3 in ARPE-19 cells transfected with empty vector or AcFLAG-SOCS3.

Supplementary Table S1 Sample information and *LINC00167* expression level.

GSM No.	Macular /Extramacular	Clinical diagnosis	Age	Gender	<i>LINC00167</i> expression
GSM738433	Macular	Normal	9	male	7.1
GSM738435	Macular	Normal	10	male	6.7
GSM738437	Macular	Normal	18	female	7.1
GSM738439	Macular	Normal	21	female	5
GSM738441	Macular	Normal	34	male	9.9
GSM738443	Macular	Normal	36	female	12.5
GSM738445	Macular	Normal	37	male	7.7
GSM738447	Macular	Normal	40	female	6.9
GSM738450	Macular	Normal	45	male	4.6
GSM738452	Macular	Normal	47	male	6.9
GSM738453	Macular	Normal	48	male	8.5
GSM738455	Macular	Normal	48	male	12.1
GSM738457	Macular	Normal	49	female	12
GSM738459	Macular	Normal	49	male	16.8
GSM738461	Macular	Normal	49	male	10.3
GSM738464	Macular	Normal	61	male	6.7
GSM738466	Macular	Normal	63	male	5.7
GSM738469	Macular	Normal	65	male	7.1
GSM738471	Macular	Normal	65	male	7.7
GSM738472	Macular	Normal	65	female	7.2
GSM738474	Macular	Normal	66	female	6.5
GSM738476	Macular	Normal	67	male	5.9
GSM738478	Macular	Normal	68	female	6.7
GSM738480	Macular	Normal	68	male	5.1
GSM738483	Macular	Normal	69	male	15.2
GSM738484	Macular	Normal	73	male	6.3

GSM738486	Macular	Normal	73	male	4.3
GSM738488	Macular	Normal	74	male	5.3
GSM738491	Macular	Normal	75	female	6
GSM738494	Macular	Normal	76	female	7.1
GSM738495	Macular	Normal	76	female	6.2
GSM738497	Macular	Normal	78	male	14.2
GSM738498	Macular	Normal	78	female	7
GSM738500	Macular	Normal	78	female	5
GSM738503	Macular	Normal	81	male	5
GSM738505	Macular	Normal	82	female	8.9
GSM738506	Macular	Normal	83	male	6
GSM738508	Macular	Normal	84	male	8.2
GSM738510	Macular	Normal	84	male	4.7
GSM738511	Macular	Normal	85	female	6.6
GSM738512	Macular	Normal	86	female	6.4
GSM738514	Macular	Normal	86	male	5.7
GSM738515	Macular	Normal	87	female	8
GSM738516	Macular	Normal	88	male	7.6
GSM738518	Macular	Normal	88	female	6.4
GSM738520	Macular	Normal	88	male	9.4
GSM738521	Macular	Normal	90	female	8
GSM738523	Macular	Normal	91	male	6
GSM738525	Macular	Normal	92	male	5.6
GSM738527	Macular	Normal	93	female	6
GSM738533	Macular	MD1	63	male	9.7
GSM738535	Macular	MD1	64	male	8.3
GSM738537	Macular	MD1	65	female	10
GSM738568	Macular	MD1	83	male	4.9
GSM738584	Macular	MD1	86	female	3.4

GSM738593	Macular	MD1	86	female	4.2
GSM738554	Macular	MD2	78	female	4.1
GSM738562	Macular	MD2	79	male	8.5
GSM738597	Macular	MD2	91	male	6.2
GSM738603	Macular	MD2	93	female	5.4
GSM738529	Macular	dry AMD	43	male	7.3
GSM738531	Macular	dry AMD	63	female	10.9
GSM738539	Macular	dry AMD	71	male	4.5
GSM738543	Macular	dry AMD	76	female	5
GSM738545	Macular	dry AMD	77	male	6.2
GSM738547	Macular	dry AMD	77	female	5
GSM738549	Macular	dry AMD	77	female	5.6
GSM738553	Macular	dry AMD	78	male	3.8
GSM738564	Macular	dry AMD	80	female	6.4
GSM738566	Macular	dry AMD	83	female	6.1
GSM738576	Macular	dry AMD	86	female	3.6
GSM738580	Macular	dry AMD	86	female	5
GSM738582	Macular	dry AMD	86	female	4.5
GSM738595	Macular	dry AMD	91	female	4.3
GSM738605	Macular	dry AMD	94	female	5.9
GSM738607	Macular	dry AMD	101	female	4.1
GSM738556	Macular	clinical AMD diagnosis	78	male	6.7
GSM738572	Macular	clinical AMD diagnosis	84	male	17.4
GSM738574	Macular	clinical AMD diagnosis	85	male	6.9
GSM738585	Macular	clinical AMD diagnosis	86	female	4.7
GSM738589	Macular	clinical AMD diagnosis	88	female	8
GSM738601	Macular	clinical AMD diagnosis	92	female	7.1
GSM738542	Macular	GA	65	female	7.4
GSM738591	Macular	GA	90	male	8.8

GSM738434	Extramacular	Normal	9	male	8.2
GSM738436	Extramacular	Normal	10	male	10.6
GSM738438	Extramacular	Normal	18	female	5.6
GSM738440	Extramacular	Normal	21	female	10.4
GSM738442	Extramacular	Normal	34	male	6.2
GSM738444	Extramacular	Normal	36	female	11.7
GSM738446	Extramacular	Normal	37	male	7.9
GSM738448	Extramacular	Normal	40	female	5.2
GSM738449	Extramacular	Normal	44	female	7.5
GSM738451	Extramacular	Normal	45	male	8.5
GSM738454	Extramacular	Normal	48	male	7.7
GSM738456	Extramacular	Normal	48	male	11.1
GSM738458	Extramacular	Normal	49	female	5.1
GSM738460	Extramacular	Normal	48	male	4.3
GSM738462	Extramacular	Normal	48	male	5.4
GSM738463	Extramacular	Normal	55	male	7
GSM738465	Extramacular	Normal	61	male	9.4
GSM738467	Extramacular	Normal	63	male	7.7
GSM738468	Extramacular	Normal	63	male	7.3
GSM738470	Extramacular	Normal	65	male	6.6
GSM738473	Extramacular	Normal	65	female	5.2
GSM738475	Extramacular	Normal	65	female	4.7
GSM738477	Extramacular	Normal	67	male	8.2
GSM738479	Extramacular	Normal	68	female	7.9
GSM738481	Extramacular	Normal	68	male	8.1
GSM738482	Extramacular	Normal	69	male	4
GSM738485	Extramacular	Normal	73	male	6.4
GSM738487	Extramacular	Normal	73	male	7
GSM738489	Extramacular	Normal	74	male	6.6

GSM738490	Extramacular	Normal	74	male	7.8
GSM738492	Extramacular	Normal	75	female	4.1
GSM738493	Extramacular	Normal	75	male	10.7
GSM738496	Extramacular	Normal	76	female	5.6
GSM738499	Extramacular	Normal	78	female	9.5
GSM738501	Extramacular	Normal	78	female	8.3
GSM738502	Extramacular	Normal	78	female	12.5
GSM738504	Extramacular	Normal	81	male	7.1
GSM738507	Extramacular	Normal	83	male	5.3
GSM738509	Extramacular	Normal	84	male	8
GSM738513	Extramacular	Normal	86	female	8.3
GSM738517	Extramacular	Normal	88	male	10.6
GSM738519	Extramacular	Normal	88	female	18.2
GSM738522	Extramacular	Normal	90	female	6.4
GSM738524	Extramacular	Normal	91	male	12.3
GSM738526	Extramacular	Normal	92	male	7.7
GSM738528	Extramacular	Normal	93	female	7.8
GSM738534	Extramacular	MD1	63	male	8.3
GSM738536	Extramacular	MD1	64	male	6
GSM738538	Extramacular	MD1	65	female	9.8
GSM738569	Extramacular	MD1	83	male	11.5
GSM738594	Extramacular	MD1	86	female	11.7
GSM738555	Extramacular	MD2	78	female	9.7
GSM738563	Extramacular	MD2	79	male	14.1
GSM738598	Extramacular	MD2	91	male	17
GSM738604	Extramacular	MD2	93	female	5.4
GSM738530	Extramacular	dry AMD	43	male	8.5
GSM738532	Extramacular	dry AMD	63	female	18.1
GSM738540	Extramacular	dry AMD	71	male	6.5

GSM738544	Extramacular	dry AMD	76	female	5.5
GSM738546	Extramacular	dry AMD	77	male	6.4
GSM738548	Extramacular	dry AMD	77	female	7.4
GSM738550	Extramacular	dry AMD	77	female	6.6
GSM738565	Extramacular	dry AMD	80	female	6.1
GSM738567	Extramacular	dry AMD	83	female	12.6
GSM738577	Extramacular	dry AMD	86	female	12.3
GSM738581	Extramacular	dry AMD	86	female	9
GSM738583	Extramacular	dry AMD	86	female	3.1
GSM738596	Extramacular	dry AMD	91	female	8.7
GSM738606	Extramacular	dry AMD	94	female	11.1
GSM738557	Extramacular	clinical AMD diagnosis	78	male	3.3
GSM738573	Extramacular	clinical AMD diagnosis	84	male	5.4
GSM738575	Extramacular	clinical AMD diagnosis	85	male	5.8
GSM738586	Extramacular	clinical AMD diagnosis	86	female	9.7
GSM738590	Extramacular	clinical AMD diagnosis	88	female	7.3
GSM738602	Extramacular	clinical AMD diagnosis	92	female	6.1
GSM738541	Extramacular	GA	64	male	7
GSM738592	Extramacular	GA	90	male	11.9

Supplementary Table S2 Sequences of mimics/inhibitors/siRNA.

mimic/inhibitor/siRNA Sequence (5'→3')

NC mimic	UUCUCCGAACGUGUCACGUTT
miR-203a-3p mimic	sense: GUGAAAUGUUUAGGACCACUAG antisense: CUAGUGGUCCUAAACAUUUCAC
miR-203a-3p inhibitor	CUAGUGGUCCUAAACAUUUCAC
scramble siRNA	sense: UUCUCCGAACGUGUCACGUdTdT antisense: ACGUGACACGUUCGGAGAAdTdT
LINC00167-siRNA	sense: GCUAUGUUCGUGAUAUCUAdTdT antisense: UAGAUAUCACGAACAUAGCdTdT
SOCS3-siRNA	sense: GACCCAGUCUGGGACCAAGdTdT antisense: CUUGGUCCCAGACUGGGUCdTdT

Supplementary Table S3 Antibodies used in this study.

Anti-protein	Host	Dilution and Application	Supplier
ZO-1	Rabbit	1:100, Immunofluorescence; 1:200, Immunoblotting	Invitrogen
β -catenin	Rabbit	1:100, Immunofluorescence; 1:1000, Immunoblotting	Cell Signaling Technology
GAPDH	Rabbit	1:1000, Immunoblotting	Bioworld
MITF	Rabbit	1:1000, Immunoblotting	Cell Signaling Technology
Keratin 18	Rabbit	1:10000, Immunoblotting	Abcam
SOCS3	Rabbit	1:1000, Immunoblotting	Proteintech
